Title	Bimetallic PdCu Nanoparticle Catalyst Supported on Hydrotalcite for Selective Aerobic Oxidation of Benzyl Alcohol
Author(s)	Nishimura, Shun; Yoshida, Nao; Ebitani, Kohki
Citation	MRS Proceedings, 1760
Issue Date	2015
Type	Conference Paper
Text version	publisher
URL	http://hdl.handle.net/10119/13506
Rights	Copyright (C) 2015 Materials Research Society. Shun Nishimura, Nao Yoshida, Kohki Ebitani, MRS Proceedings, 1760, 2015, DOI:10.1557/opl.2015.58. http://dx.doi.org/10.1557/opl.2015.58
Description	

Mater. Res. Soc. Symp. Proc. Vol. 1760 © 2015 Materials Research Society
DOI: 10.1557/opl.2015.58

Bimetallic PdCu Nanoparticle Catalyst Supported on Hydrotalcite for Selective Aerobic Oxidation of Benzyl Alcohol

Shun Nishimura,[1] Nao Yoshida[1] and Kohki Ebitani[1,*]
[1] School of Materials Science, Japan Advanced Institute of Science and Technology, 1-1 Asahidai, Nomi, Ishikawa 923-1292, Japan.

ABSTRACT

To decrease the amount of precious metal usage for Pd-catalyzed aerobic alcohol oxidation, various amount of Cu-contained Pd bimetallic nanoparticle-supported solid base hydrotalcite catalyst (Pd_xCu_y-PVP/HTs) were prepared and applied for aerobic benzyl alcohol oxidation. It was found that the addition of Cu atoms into Pd in the range of 0-40% provided a similar or a little superior activity to that of Pd_{100}-PVP catalyst, whereas a large quantity of co-existence Cu (>40%) gradually decreased their activity of the catalyst. The aerobic benzyl alcohol oxidation over $Pd_{80}Cu_{20}$-PVP/HT served 77% yield and 95% selectivity towards benzaldehyde at 313 K for 5 h in toluene under O_2 flow. X-ray adsorption spectroscopy (XAS) studies and scanning transmission electron microscopy-high angle annuar dark field (STEM-HAADF) with energy dispersive X-ray spectroscopy (EDS) analyses suggested that Cu atoms doping into Pd(0) NP influenced not only localized nanostructure but also oxidation state around Pd atoms. We suggested that substitution of precious metal with small amount of transition metals such as Cu lead to geometric/electronic changes in active sites would be one of nice strategies for reducing the cost for the catalyst in the oxidation process.

INTRODUCTION

Selective oxidation of alcohols is one of the important industrial reactions for fine chemicals production; it serves key intermediates such as aldehydes, ketones and carboxylic acids. Stoichiometric oxidation processes using homogeneous oxidants such as $KMnO_4$, $K_2Cr_2O_7$ and TEMPO or metal-complex catalyzed oxidation process [1,2] have a long history for the oxidation reactions. However, these conventional processes have serious disadvantages derived from salts formation, catalyst separation and purification after product formation.

For building more environmentally-friendly chemical process, heterogeneous catalytic systems for aerobic alcohol oxidation have been studied by several groups [3,4]; it provides only water as co-product after reaction in theory, and the catalyst was easily separated from the reaction mixture. Especially in this area, precious metals (*i.e.* Au, Pd, Pt, Ru etc) based catalysts have been studied widely for the oxidation reaction [5], however, utilization of the precious metal needs to be minimized in order to replace these precious catalysts for the classical process in industrial plant scales.

In this study, we focused on the transition metal Cu incorporated Pd catalyst. The PdCu bimetallic catalyst has been widely applied for hydration of acrylonitrile to acrylamide, hydrogenation of 1,3-cyclooctadiene, Sonogashira cross-coupling, CO oxidation, NO reduction and so on [6-9]. Because the nanohybrid materials composed with transition metal and precious metal are found to be nice catalyst for benzyl alcohol oxidation (*ex.* AuCu and PtCu catalysts)

[10-12], this approach focusing on PdCu catalyst would effectively contribute to the advanced technology for alcohol oxidation over heterogeneous precious metal with low loadings of Pd.

EXPERIMENTS

The poly(*N*-vinylpyrrolidone) (PVP)-protected bimetallic Pd_xCu_y nanoparticles supported onto hydrotalcite (HT) with different Pd/Cu ratio were prepared according to the previous report [8] with some modifications according to our previous method [13]. xPd(OAc)$_2$ (WAKO), yCu(OAc)$_2$•H$_2$O (KANTO) and 0.425 g of PVP (KANTO, K = 30) were added into 50 mL of 2-ethoxyethanol (WAKO) under vigorous stirring, and then heated at 413 K for 2 h to serve Pd_xCu_y-PVP nanocolloids ($x + y = 0.1$ mmol (const.)). Thereafter, 1.0 g of solid base HT (TOMITA, Mg/Al = 5.4) was added into the suspension, and treated for additional 1 h under the same temperature. The obtained emulsion was filtered and washed with deionized water (3 L), and then the collected precipitates were dried in vacuum at room temperature, affording the Pd_xCu_y-PVP/HT catalyst.

Characterizations were performed by X-ray diffraction (XRD; Shimadzu SmartLabo, Cu K_α), transmission electron microscopy (TEM; Hitachi H-7650, 100 kV), scanning-TEM-high angle annuar dark field (STEM-HAADF) with energy dispersive X-ray spectroscopy (EDS) and inductively-coupled plasma (ICP-AES; Shimadzu ICPS-7000 ver.2). X-ray adsorption spectroscopy (XAS) was obtained at a BL01B1 in SPring-8 (Harima, Japan) for Pd-K edge (Proposal No. 2014B1036).

The benzyl alcohol oxidation was examined in a round-bottle glass flask (20 mL vol.) attached with a condenser. In a typical operation, the mixtures of Pd_xCu_y-PVP/HT catalyst (0.2 g) and benzyl alcohol (2 mmol) dispersed in toluene solvent (5 mL) were putted into a 313 K oil bath and kept for setting time under O_2 flow (20 mL•min^{-1}) with vigorous stirring (450 rpm). The product was analyzed by a GC-FID chromatography (Shimadzu GC-2014) with a polar column (Agilent DB-FFAP, 30 m). The naphthalene (TCI) was used as an internal standard.

DISCUSSION

The XRD patterns of all Pd_xCu_y-PVP NPs samples, the dried powders obtained from as-prepared Pd_xCu_y-PVP nanocolloids, exhibited no significant peaks except for the broadening peak at 2θ = 20-30 degree attributed to PVP polymer protecting agents (The data were not shown here). Thus, there were no aggregates of Pd and/or Cu metal particles in the nanocolloids. It was reported that nano-sized Pd(0)-PVP NPs below *ca.* 25 nm in diameter possessed low crystallinity (amorphous) [14], thus XRD technique seems to be inadequate for Pd_xCu_y-PVP NPs.

TEM images of Pd_xCu_y-PVP/HT samples are shown in Figures 1 with particles size distribution. In all cases, the reticulated structures of HT itself were observed. It was hard to calculate the size distribution in high Cu contents of Cu_{100}-PVP/HT and $Pd_{20}Cu_{80}$-PVP/HT because of difficulty in observations of clear particles at many spots. Among Pd_xCu_y-PVP/HTs with Cu contents of 0-60%, the size distributions were narrow and Ave. diameter was at 3-4 nm.

As-prepared Pd_xCu_y-PVP/HTs with various Pd/Cu mole ratios were applied for benzyl alcohol oxidation in toluene using O_2 gas flow as oxidant. The initial activities of each Pd_xCu_y-PVP/HT catalyst as a function of Cu contents were plotted in Figure 2. The Pd_{100}-PVP/HT was

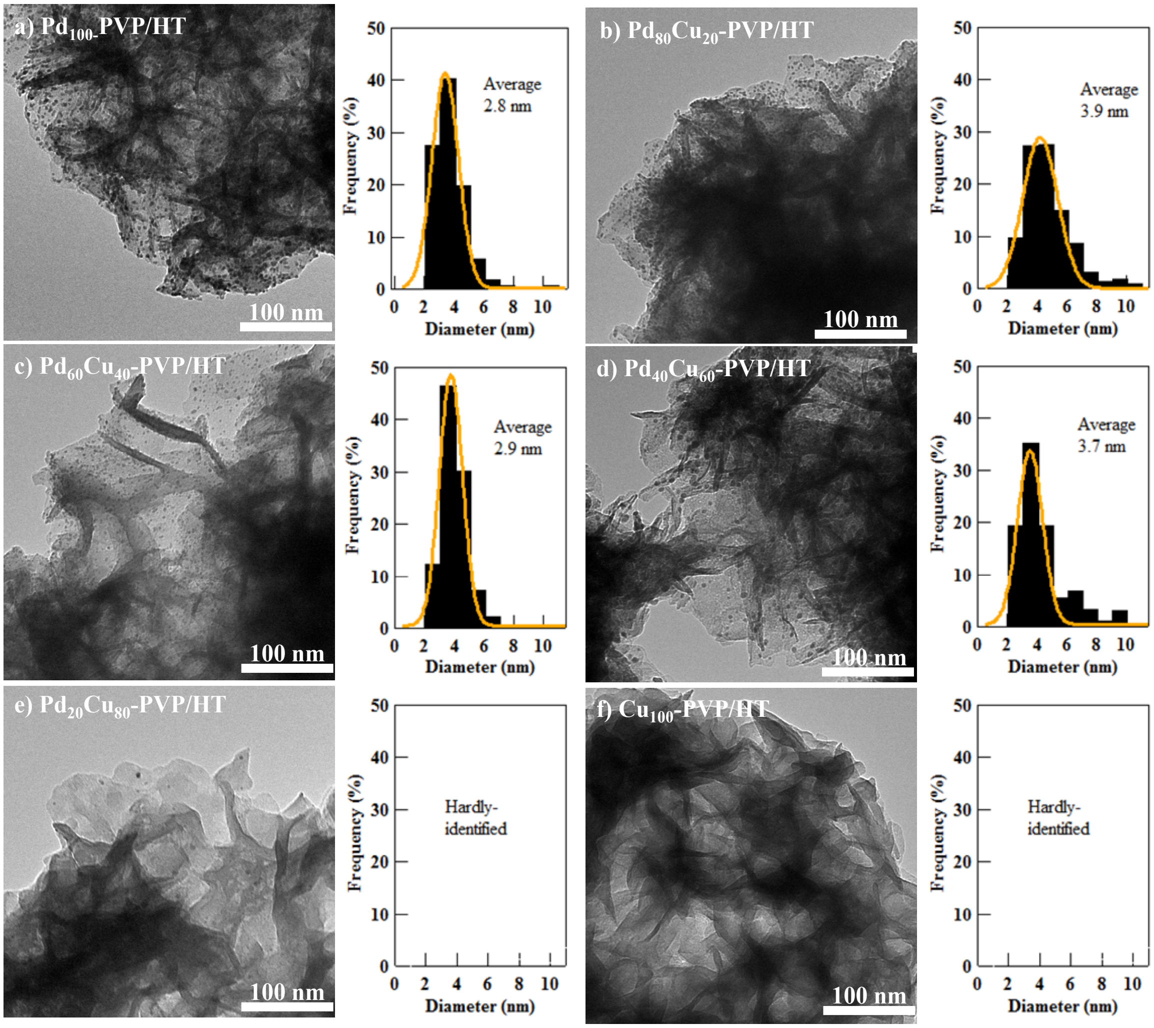

Figure 1. TEM images of Pd_xCu_y-PVP/HT with particle size distributions.

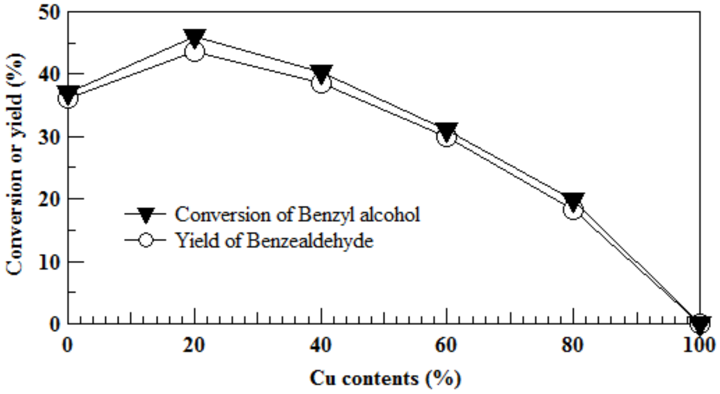

Figure 2. Activities for aerobic oxidation of benzyl alcohol toward benzaldehyde over Pd_xCu_y-PVP/HT catalysts in toluene for 1 h at 313 K.

active (36% yield) whereas Cu$_{100}$-PVP/HT was completely inactive (0% yield) under the same reaction condition. A little Cu substitution into Pd (40%) kept the activity of approximately 40% yields of benzaldehyde, thereafter, the yield was gradually decreased with increases of Cu contents. The mean diameter of 2.8 nm, 3.9 nm, and 2.9 nm was determined for Pd$_{100}$-PVP/HT, Pd$_{80}$Cu$_{20}$-PVP/HT, and Pd$_{60}$Cu$_{40}$-PVP/HT, respectively, as described in Figure 1. Thus, it is likely that the particle size of Pd$_x$Cu$_y$-PVP NPs stabilized on HT scarcely contributed to its activity. ICP results indicated that the actual amounts of Pd and Cu elements in these three catalysts were almost similar values to the theory; *i.e.* Pd$_{100}$-PVP/HT (Pd: 0.095 mmol/g), Pd$_{79.3}$Cu$_{20.7}$-PVP/HT (Pd; 0.073 mmol/g, Cu; 0.019 mmol/g), and Pd$_{58.5}$Cu$_{41.5}$-PVP/HT (Pd; 0.055 mmol/g, Cu; 0.039 mmol/g) were determined as the actual ratio, respectively.

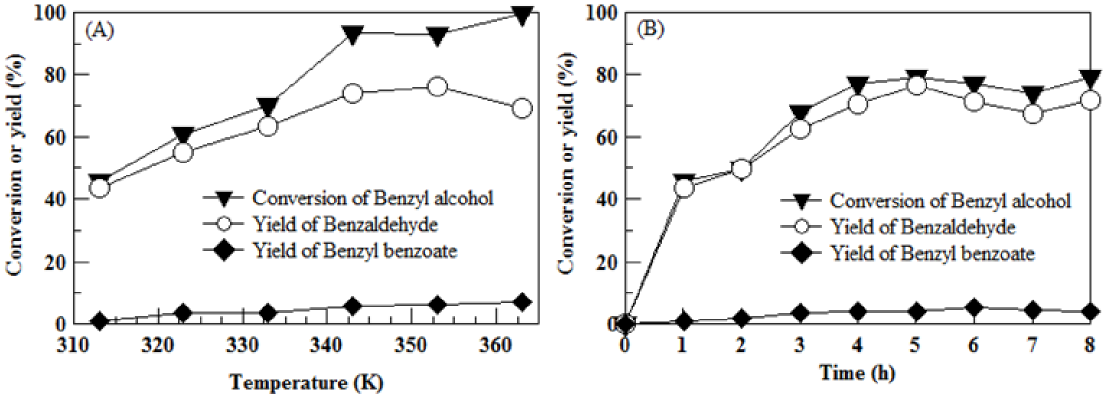

Figure 3. Effects of (A) Reaction temperature for 1 h reaction and (B) Reaction time at 313 K on aerobic oxidation of benzyl alcohol over Pd$_{80}$Cu$_{20}$-PVP/HT catalyst.

Effects of reaction temperature and time were monitored by using Pd$_{80}$Cu$_{20}$-PVP/HT, as shown in Figures 3(A) and (B). The yield of benzaldehyde was increased to 76% when the reaction temperature increased. However, it seems that the over-oxidations to benzyl benzoate and other by-products were also accelerated at the same time leading to decrease of the selectivity for benzaldehyde drastically. While, both the high yield and selectivity for benzaldehyde were achieved by elongating the time to 5 h in the time-course at 313 K, affording to 77% yield with 95% selectivity.

To estimate the changes in Pd atoms by Cu substitution, XAS studies were performed in the Pd K-edge (see Figures 4). The Pd K-edge XANES features showed Pd metallic state was dominant in all Pd$_x$Cu$_y$-PVP/HT. The |FT| of k^3-weighted Pd K-edge EXAFS indicated that Cu induced significant changes in Pd(0) location; the peak broadening and shifts to lower distance were observed with increase of Cu amount. For Pd$_{80}$Cu$_{20}$-PVP/HT and Pd$_{20}$Cu$_{80}$-PVP/HT, the

Table 1. Curve-fitting parameters in the |FT| of k^3-weighted Pd-K edge EXAFS spectra.

Samples	**Shell**	**Coordination number**	**Distance (Å)**	**Debye–Waller factor (Å^2)**	**R factor (%)**
Pd$_{80}$Cu$_{20}$-PVP/HT	Pd-Pd	7.5	2.73	0.0104	0.6
	Pd-Cu	0.9	2.65	0.0017	
Pd$_{20}$Cu$_{80}$-PVP/HT	Pd-Pd	5.5	2.70	0.0064	0.8
	Pd-Cu	5.9	2.68	0.0100	

curve-fitting analysis was performed in the range of k = 4-14 Å^{-1} with inverse FT in R = 1.719-2.946 Å. The calculated values with curve-fitting (McKale) were listed in Table 1 and described in Figure 4(B) as red lines. It was suggested that the Pd-Cu coordination was presence in Pd_xCu_y-PVP/HT catalysts, which influenced on changes in the Pd-Pd distances and/or structure of active sites (*ex.* PdCu alloying). Previously, in the PdCo catalysts, it was reported that incorporated Co atoms into Pd NPs caused changed in Pd-Pd interatomic distance and/or electronic states of d states more favorable for catalysis [15-16]. Thus, we supposed that a little Cu substitution into Pd NPs induced Pd-Cu alloy formation partially, and resulted in more favorable geometric/electronic states in Pd sites for aerobic alcohol oxidation reaction.

In order to identify the nanostructure of as-prepared PdCu NPs, STEM-HADFF images with EDS elemental mapping analysis were performed on the $Pd_{60}Cu_{40}$-PVP NPs as shown in Figure 5. Both images at low and high magnification nicely indicated that each NP was composed by both Pd and Cu elements, *i.e.* Cu-Pd alloying.

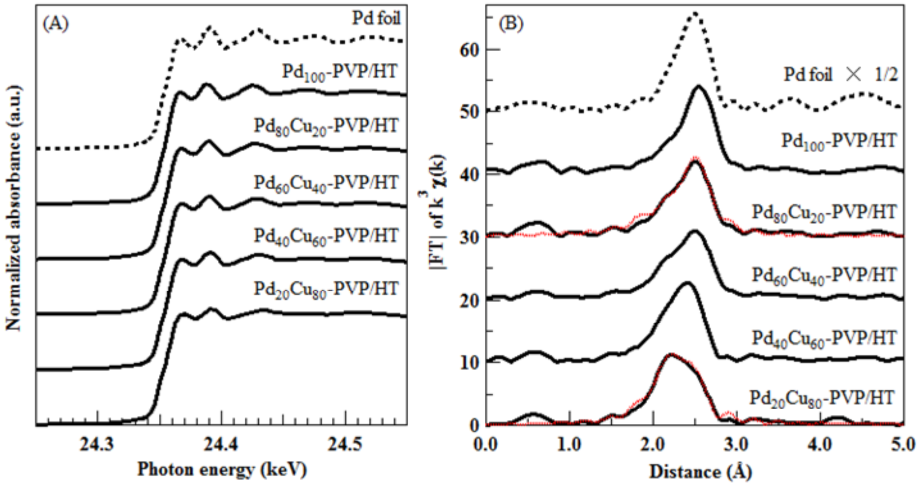

Figure 4. Pd K-edge XAS results in (A) XANES and (B) |FT| of k^3-weighted EXAFS applied in the range of k = 3-15 Å^{-1}. The McKale fitting results are shown as the red dash lines in (B).

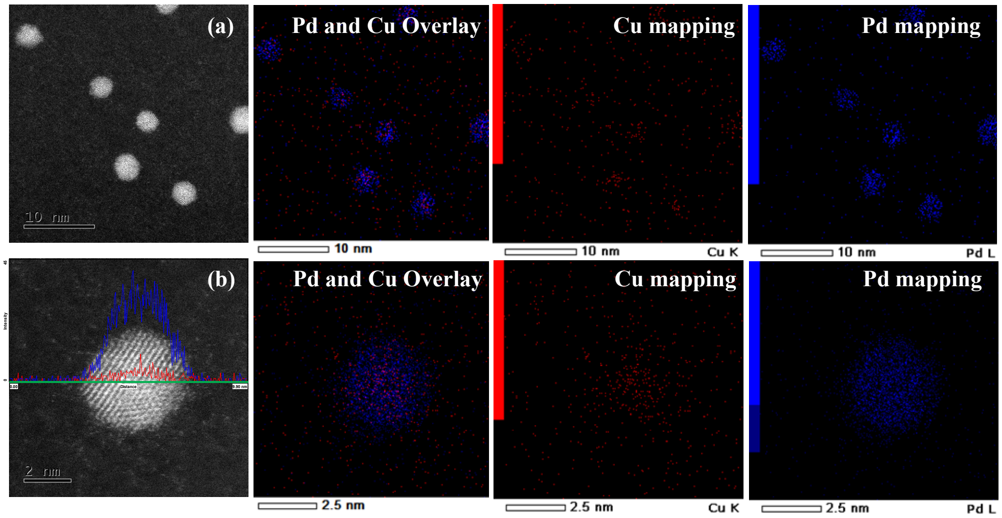

Figure 5. STEM-HADFF images and EDS-mapping results of $Pd_{60}Cu_{40}$-PVP NPs in different magnifications. The blue and the red line in image (b) was Pd and Cu distribution, respectively, determined by an EDS-line analysis on the green line.

CONCLUSIONS

The Pd_xCu_y-PVP/HT prepared with various Pd/Cu molar ratios were applied for aerobic oxidation of benzyl alcohol to benzaldehyde in toluene at 313 K. It was observed that Cu contents in Pd_xCu_y-PVP/HT catalyst contributed to the activity, and a little amount of Cu (0-40%) was effective for reducing Pd uses with similar catalytic performance with Pd itself (Pd_{100}-PVP/HT). We supposed that substituted Cu with Pd atoms changed geometric/electronic location around Pd atoms, and then promoted the catalysis over Pd_xCu_y-PVP/HT even with low loading of Pd. Further work on nanostructure and catalysis of PdCu-PVP/HT are ongoing.

ACKNOWLEDGMENTS

This work was partly supported by a Grant-in-Aid for Young Scientists (B) (25820392) of the Ministry of Education, Culture, Sports, Science and Technology (MEXT), Japan, and a cooperative work General C (H26-No.29) in Materials and Structures Laboratory, Tokyo Institute of Technology. We appreciate Dr. Kohichi Higasimine (JAIST, Nano-center) for his great help on STEM-HAADF and EDS mapping analyses.

REFERENCES

1. A. Dijksman, A. Marino-Gozalez, A. M. I Payeras, I. W. C. E. Arends and R. A. Sheldon, *J. Am. Chem. Soc.* **123**, 6826 (2001).
2. E. Balaraman, E. khaskin, G. Leitus and D. Milstein, *Nature Chem.* **5**, 122 (2013).
3. T. Mallat and A. Baiker, *Chem. Rev.* **104**, 3037 (2004) (review).
4. S. E. Davis, M. S. Ide and R. J. Davis, *Green Chem.* **15**, 17 (2013) (review)
5. A. F. Lee, "Mechanistic Studies of Alcohol Selective Oxidation", *Heterogeneous Catalysts for Clean Technology: Spectroscopy, Design, and Monitoring*, ed. K. Wilson and A. F. Lee (Wiley 2013) pp.11-38.
6. N. Toshima and Y. Wang, *Langmuir* **10**, 4574 (1994).
7. D. Sengupta, J. Saha, G. De and B. Basu, *J. Mater. Chem. A* **2**, 3986 (2014).
8. K. A. Guy, H. Xu, J. C. Yang, C. J. Werth and J. R. Shapley, *J. Phys. Chem. C* **113**, 8177 (2009).
9. V. Mazumder, M. Chi, M. N. Mankin, Y. Liu, O. Metin, D. Sun, K. L. More, S. Sun, *Nano Lett.* **12**, 1102 (2012).
10. D. Liang, J. Gao, J. H. Wang, P. chen, Y. F. Wei, Z. Y. Hou, *Catal. Commun.* **12**, 1059 (2011).
11. C. D. Pina, E. Falletta and M. Rossi, *J. Catal.* **260**, 384 (2008).
12. Q. Q. Jia, D. F. Zhao, B. Tang, N. Zhao, H. D. Li, Y. H. Sang, N. Bao, X. M. Zhang, X. H. Xu, H. Liu, *J. Mater. Chem. A* **2**, 38 (2014).
13. S. Nishimura, Y. Yakita, M. Katayama, K. Higashimine and K. Ebitani, *Catal. Sci. Technol.* **3**, 351 (2013).
14. J. S. Bradley, E. W. Hill, S. Behal and C. Klein, *Chem. Mater.* **4**, 1234 (1992).
15. S. Takehira, T. Tsukamoto, H. Matsune, and M. Kishida, *Catal. Sci. Technol.* **3**, 2723 (2013).
16. W. G. Menezes, L. Altmann, V. Zielasek, K. Thiel, M. Baumer, *J. Catal.* **300**, 125 (2013).